

# AN EXPERIMENTAL COMPARISON OF A SPACE-TIME MULTIGRID METHOD WITH PFASST FOR A REACTION-DIFFUSION PROBLEM

PIETRO BENEDUSI\*, MICHAEL L. MINION†, AND ROLF KRAUSE\*

**Abstract.** We consider two parallel-in-time approaches applied to a (reaction) diffusion problem, possibly non-linear. In particular, we consider PFASST (Parallel Full Approximation Scheme in Space and Time) and space-time multilevel strategies. For both approaches, we start from an integral formulation of the continuous time dependent problem. Then, a collocation form for PFASST and a discontinuous Galerkin discretization in time for the space-time multigrid are employed, resulting in the same discrete solution at the time nodes. Strong and weak scaling of both multilevel strategies is compared for varying order of the temporal discretization. Moreover, we investigate the respective convergence behavior for non-linear problems and highlight quantitative differences.

**Key words.** space-time multigrid, PFASST, parallel-in-time, DG discretization, strong and weak scalability, reaction-diffusion equation

**AMS subject classifications.** 65F10, 65L60, 65N55, 65M70, 65Y05

**1. Introduction.** Since the clock frequency of computer processors has not increased significantly in the past fifteen years, an increase in computational performance for numerical algorithms can be achieved only by increasing parallel concurrency, and modern supercomputers now contain many thousands of computing cores. Exploiting the capabilities of such massively parallel systems is not straightforward; algorithms with optimal complexity and excellent scalability must be designed to minimize the run-time of computationally intensive problems, such as the solution of time dependent partial differential equations (PDEs). When dealing with parallel solvers for discretized PDEs, the solution process is traditionally parallelized in space using domain decomposition techniques, until stagnation. Considering the technology trend, the traditional sequential time stepping will increasingly become the bottleneck for computational scalability. Hence, the development of new parallel methods that exploit concurrency in the time direction has become essential for time dependent problems. However, parallelization in time can be a challenging task, as, for many physical processes, the time direction is governed by a causality principle, with a preferential direction of information flow through the temporal domain, i.e. forward in time. Nevertheless, several new methods for temporal parallelization have been proposed in the last 20 years. For a more comprehensive review regarding the parallel-in-time literature of the past 50 years we refer to [22].

The objective of this work is to compare two of the most relevant recent approaches: PFASST [14] and space-time multigrid methods (STMG) [26, 29, 18, 24, 21, 6]. The current paper is similar in spirit to the comparison presented in [19] (where the authors suggest a future comparison with PFASST). Since many parallel-in-time methods are based on a coupling between coarse and fine time propagators, they can

---

\*Institute of Computational Science, University of Italian Switzerland (USI), Lugano, Switzerland (pietro.benedusi@usi.ch, rolf.krause@usi.ch).

†Lawrence Berkeley National Laboratory, Berkeley, CA (MLMinion@lbl.gov).

be framed in a multilevel-in-time setting; for example, MGRIT [18], Parareal in [23] or PFASST in [8]. Despite the similarities of these different approaches, the methods can behave quite differently on some problems. To date, the majority of papers on parallel in time methods investigate a single method, and very few have investigated the computational advantages and disadvantages of different methods on well defined benchmarks.

In the remainder of this paper we present such a comparison between PFASST and STMG. In Section 2 we describe the respective time discretizations of the two approaches. In Section 3 we present a reaction-diffusion PDE and its discretization in space and time. In Section 4 we describe the solution methods that will be used in Section 5, where weak and strong scaling experiments are reported.

**2. Preliminaries on the time discretizations.** Let us introduce the time discretizations that we use for PFASST and the space-time multigrid (STMG), respectively. Both formulations are equivalent to the same implicit Runge-Kuta (RK) method and are based on an integral form of the continuous problem. To illustrate these methods we consider the initial value problem on a single time step  $I_n := [T_n, T_{n+1}] \subset \mathbb{R}$

$$(2.1) \quad u'(t) = f(u(t), t) \quad \text{for } T_n < t < T_{n+1}, \quad u(T_n) = U_0.$$

**2.1. Collocation form.** The PFASST algorithm is based on the spectral deferred correction (SDC) method, an iterative scheme introduced in [13] based on a collocation approximation of (2.1). Let us consider the Picard integral form of (2.1)

$$(2.2) \quad u(t) = U_0 + \int_{T_n}^t f(u(\tau), \tau) d\tau,$$

and the  $M$  right Gauss-Radau nodes  $\{t_m\}_{m=1}^M$  in  $I_n$  with  $T_n < t_1 < t_2 < \dots < t_M = T_{n+1}$ . We approximate (2.2) by its collocation form, with  $U_m \approx u(t_m)$ :

$$(2.3) \quad \mathbf{U} = \mathbf{U}_0 + \Delta t Q F(\mathbf{U}),$$

where  $\Delta t := T_{n+1} - T_n$ ,

$$(2.4) \quad \mathbf{U} := [U_1, \dots, U_M], \quad \mathbf{U}_0 := [U_0, \dots, U_0], \quad F(\mathbf{U}) := [f(U_1, t_1), \dots, f(U_M, t_M)],$$

$Q$  is the  $M \times M$  matrix  $Q := (q_{m,j})_{m,j=1}^M$  with the quadrature weights

$$q_{m,j} := \frac{1}{\Delta t} \int_{T_n}^{t_m} \ell_j(t) dt,$$

and  $\{\ell_j\}_{j=1}^M$  are the Lagrange polynomials at the  $M$  nodes. An SDC iteration can be considered as a preconditioned Richardson iteration to solve (2.3) (see, e.g. [30, 49]) and, if SDC converges, it is equivalent to an implicit (RK) method, with  $q_{m,j}$  being the values in the corresponding Butcher tableaux. The resulting RK method is  $A$ -stable and has order of accuracy  $2M - 1$  for  $M$  Radau quadrature nodes [27].

**2.2. Discontinuous Galerkin.** Variational time-stepping methods are receiving increasing interest by the scientific community, especially in the context of adaptivity in spacetime, for example in [15, 42]. Discontinuous Galerkin (DG) methods, in particular, have been widely used to discretize the time direction in the space-time setting as they ensure that the information flows in the positive time direction. They have been employed for a variety of problems such as convection/advection/diffusion equations or the Navier-Stokes equations. For example see the work of [32, 34, 36, 47, 20, 7, 24, 5]. The use of DG discretization in time was first introduced in [35] for the discretization of a neutron transport equation. In this paper the authors showed that, for finite elements of order  $q$ , the method is strongly  $A$ -stable, has convergence order  $2q + 1$  in the nodes, and is equivalent to an implicit (RK) time stepper with  $q$  intermediate steps. The first analysis on DG methods as time stepping techniques was provided by [12] and [17], followed by the work of [41, 50, 48]. More recently, specialized solution methods have been introduced, for example by [45, 40, 31, 4]. A *priori* and *posteriori* error analysis have been also provided, e.g. see [48, 15, 16, 43]. See [44] for a recent survey on the topic.

Let us consider the weak formulation of (2.1), where the continuity at  $T_n$  is weakly imposed, and  $u \approx U \in \mathbb{P}_q(I_n)$

$$(2.5) \quad \int_{T_n}^{T_{n+1}} U'(t)v(t) dt + (U(T_n) - U_0)v(T_n) = \int_{T_n}^{T_{n+1}} f(U(t), t)v(t) dt,$$

for every test functions  $v \in \mathbb{P}_q(I_n)$ . Equivalently, integrating by parts (2.5), we obtain the standard DG formulation:

$$(2.6) \quad - \int_{T_n}^{T_{n+1}} U(t)v'(t) dt + U(T_{n+1})v(T_{n+1}) - v(T_n)U_0 = \int_{T_n}^{T_{n+1}} f(U(t), t)v(t) dt,$$

where we highlight the *upwind flux* given by the  $v(T_n)U_0$  term. In the interval  $I_n$ , we construct the approximation  $U$  in the nodal form,

$$(2.7) \quad U(t) = \sum_{m=1}^M U_m \ell_{n,m}(t),$$

where  $\{\ell_{n,m}\}_{m=1}^M$  is the basis of Lagrange polynomials of degree  $q$  at the  $q + 1 = M$  Gauss-Radau nodes in  $I_n$ . We can rewrite (2.6), using the approximation in (2.7) and the definitions in (2.4), as

$$(2.8) \quad K_q \mathbf{U} = J_q \mathbf{U}_0 + M_q F(\mathbf{U}),$$

with

$$(2.9) \quad K_q := \left[ - \int_{T_n}^{T_{n+1}} \ell'_{n,i}(t) \ell_{n,j}(t) dt + \ell_{n,i}(T_{n+1}) \ell_{n,j}(T_{n+1}) \right]_{i,j=1}^M,$$

$$(2.10) \quad M_q := \left[ \int_{T_n}^{T_{n+1}} \ell_{n,i}(t) \ell_{n,j}(t) dt \right]_{i,j=1}^M, \quad J_q := [\ell_i(T_n) \ell_j(T_{n+1})]_{i,j=1}^M.$$

Let us remark the similarity between (2.3) and (2.8) and that  $J_q \mathbf{U}_0 = [U_0, 0, \dots, 0]^T$ . For multiple adjacent time elements equation (2.8) can be naturally extended, with obvious notation, as

$$(2.11) \quad K_q \mathbf{U}_n = J_q \mathbf{U}_{n-1} + M_q F(\mathbf{U}_n).$$

**3. Problem setting and discretization.** Let  $\Omega = (0, X)$  be the spatial domain and  $T \in \mathbb{R}^+$  the final time. We consider the following non-linear reaction diffusion equation:

$$(3.1) \quad \begin{cases} \partial_t u - \partial_{xx} u + \gamma(u^3 - u) = 0, & \text{for } (t, x) \in (0, T) \times \Omega, \\ \partial_x u = 0, & \text{for } (t, x) \in (0, T) \times \partial\Omega, \\ u = u_0, & \text{for } t = 0 \text{ and } x \in \Omega, \end{cases}$$

where  $u := u(t, x)$ ,  $u_0 := u_0(x)$ , and  $\gamma \geq 0$  controls the intensity of the reaction term. Equation (3.1) is known as the monodomain model and it is used to describe the progressive activation of excitable media. For example, in the context of computational medicine, it is employed to simulate the propagation of the electrical potential in the human heart [33]. The cubic term is a FitzHugh-Nagumo-type reaction, with three zeros  $\{-1, 0, 1\}$  corresponding, respectively, to a resting state, a threshold and an activation state. For  $\gamma = 0$  equation (3.1) is reduced to the heat equation.

Let  $N_t, N_x \in \mathbb{N}$  be the number of time and space elements respectively, and define the following uniform partitions in time and space:

$$\begin{aligned} t_i &:= i\Delta t, & i &= 0, \dots, N_t, & \Delta t &:= T/N_t, \\ x_j &:= jh, & j &= 0, \dots, N_x, & h &:= X/N_x. \end{aligned}$$

In space, we approximate (3.1) with linear finite elements, constructing the discrete operators

$$(3.2) \quad K_h := \left[ \int_{\Omega} \varphi'_i(x) \varphi'_j(x) dx \right]_{i,j=1}^{N_x}, \quad M_h := \left[ \int_{\Omega} \varphi_i(x) \varphi_j(x) dx \right]_{i,j=1}^{N_x},$$

using the linear Lagrange basis functions  $\{\varphi_i\}_{i=1}^{N_x} \subset H^1(\Omega)$ . Referring to Section 2.2, we can consider a space-time finite element approximation of (3.1) in  $[t_n, t_{n+1}]$  with a tensor structure:

$$(3.3) \quad u(x, t) \approx U(x, t) = \sum_{i=1}^{N_x} \sum_{j=1}^M u_{i,j}^{n+1} \varphi_i(x) \ell_{n,j}(t),$$

and assemble the non-linear space-time system of size  $(N_x + 1)N_t M$

$$(3.4) \quad \begin{bmatrix} A_{h,q} & & & & \\ B_{h,q} & A_{h,q} & & & \\ & & \ddots & & \\ & & & \ddots & \\ & & & & B_{h,q} & A_{h,q} \end{bmatrix} \begin{bmatrix} \mathbf{u}_1 \\ \mathbf{u}_2 \\ \vdots \\ \mathbf{u}_{N_t} \end{bmatrix} + \gamma(I_{N_t} \otimes M_{h,q}) \begin{bmatrix} r(\mathbf{u}_1) \\ r(\mathbf{u}_2) \\ \vdots \\ r(\mathbf{u}_{N_t}) \end{bmatrix} = \begin{bmatrix} -B_{h,q} \mathbf{u}_0 \\ \mathbf{0} \\ \vdots \\ \mathbf{0} \end{bmatrix},$$

with

$$(3.5) \quad A_{h,q} := M_h \otimes K_q + K_h \otimes M_q, \quad B_{h,q} := -M_h \otimes J_q, \quad M_{h,q} := M_h \otimes M_q,$$

$I_{N_t}$  being the identity of size  $N_t$ . For  $n = 1, \dots, N_t$ , we have the solution vector

$$(3.6) \quad [\mathbf{u}_n]_{i+(j-1)M} := u_{i,j}^n \quad \text{for } i = 0, \dots, N_x \quad \text{and } j = 1, \dots, M,$$

and the point-wise reaction

$$(3.7) \quad [r(\mathbf{u}_n)]_k := [\mathbf{u}_n]_k^3 - [\mathbf{u}_n]_k \quad \text{for } k = 0, \dots, N_x M.$$

The initial condition is imposed through  $\mathbf{u}_0 := [0, \dots, 0, u_0(x_0), u_0(x_1), \dots, u_0(x_{N_x})]$ , having  $(N_x + 1)(M - 1)$  zeros. For a detailed description of the weak formulation of (3.1) (for  $\gamma = 0$ ), the assembly and spectral analysis of system (3.4), in a more general finite element framework, we refer to [5]. The storage of such a large system is expensive in terms of memory, but can be convenient if a large number of cores is employed. Let us remark that we assemble the space-time system (3.4) just in the space-time multigrid case; when using PFASST the assembly of the spatial operators in (3.2) is sufficient. For technical limitations related to the current PFASST implementation, we replace the mass matrix  $M_h$  with its lumped version for both discretizations.

**4. Solution methods.** Let us introduce the two solution strategies that will be the object of the comparison.

**4.1. PFASST.** The parallel full approximation scheme in space and time (PFASST) was introduced by Emmett and Minion in 2012 [14]. As the name suggests, PFASST can be described in the context of a multigrid in time method based on a FAS correction on coarse levels [8]. An alternative perspective on how the PFASST method is organized is to view it as a way to perform SDC iterations for the collocation Eq. (2.3) on multiple time steps simultaneously. For parallel efficiency, the SDC iterations are done on a hierarchy of levels as in the multilevel SDC method [46] with communication of new initial conditions passed forward in time between processors after each SDC iteration on each level. Since the communication is only serial on the coarsest level, the SDC iterations on the finest level are done concurrently, resulting in a potential parallel speedup if the total number of PFASST iterations needed to converge on all the time steps remains relatively small. One advantage of viewing PFASST from this SDC perspective is that variants of the original SDC method such as semi-implicit SDC (SISDC) [38], can be easily used in the PFASST context. SISDC methods (also known as implicit-explicit or IMEX) are appropriate for differential equations for which the right hand side of (2.1) can be split into stiff and non-stiff parts. These methods are often employed in situations where the non stiff component is nonlinear and the stiff term is linear, so that only a linear implicit equation needs to be solved in each time step. In Section 5.4, an IMEX treatment is used to treat the nonlinear reaction terms explicitly and the linear diffusion terms implicitly.

**4.2. Space-time multigrid.** Specialized parallel solvers have been recently developed for large linear systems arising from space-time discretizations. We mention

in particular the parallel STMG proposed by [24], the parallel preconditioners for space-time isogeometric analysis proposed by [28] and [4] as well as the block preconditioned GMRES by [37]. When dealing with a space-time discretization, where time is somehow considered as an additional spatial dimension, it is natural to extend the same paradigm for the solving process and consider space-time multigrid type algorithms.

Multigrid solvers are optimal preconditioners for elliptic problems but they have proven to be efficient, with some precautions, also for space-time discretizations of parabolic problems. In particular, the heat equation is first order in time and its discretization introduces non symmetric off-diagonal entries in the space-time system (3.4).

When dealing with anisotropic problems standard multigrid convergence rates deteriorate; see, e.g., [11]. Traditionally there are various ways to address this problem such as incorporating the asymmetry in the particular choice of line smoothers and/or adopting a semi-coarsening strategy. In [29, 23, 21, 3], for example, the authors explain how the STMG convergence depends critically on the ratio  $\mu := \Delta t/h^2$ , unless semi-coarsening strategies are adopted. In particular, for  $\mu \ll 1$  (resp.  $\mu \gg 1$ ) coarsening only in time (resp. space) is an effective strategy.

Let us consider a hierarchy of  $L$  space-time grids denoted with  $l = 1, \dots, L$  and  $l = L$  corresponding to the coarsest one. We construct the space-time restriction operator  $I_l^{l+1}$  from level  $l$  to level  $l + 1$  as

$$(4.1) \quad I_l^{l+1} = T_l^{l+1} \otimes S_l^{l+1} \otimes M_l^{l+1}, \quad \text{for } l = 1, \dots, L - 1,$$

where  $T_l^{l+1}$  and  $S_l^{l+1}$  are restriction operators in time and space respectively and  $M_l^{l+1}$  is responsible for  $M$ -coarsening in time, reducing  $M$  along the multilevel hierarchy. Definitions of these operators will be provided in the next section. Let us mention that any restriction operator in (4.1) can be replaced by a suitable identity matrix, resulting in various semi-coarsening strategies. For smoothing, we employ a GMRES solver, preconditioned with an incomplete LU factorization (PGMRES). More specialized preconditioners and corresponding tensor solvers could also be applied to system (3.4); see, e.g., [39, 9, 4]. If  $\gamma \neq 0$ , equation (3.4) is non-linear and the STMG algorithm is encapsulated in a Newton iteration.

## 5. Experiments.

**5.1. Implementation.** For the numerics of this section, as well as throughout this paper, we used the C++ frameworks PETSc [1, 2] and the embedded domain specific language Utopia<sup>1</sup> [51] for the parallel linear algebra and the linear and non-linear solvers. For PFASST we use the Fortran library LibPFASST<sup>2</sup> that was extended to use PETSc data structures to make the comparison as fair as possible. The two discretizations produce, up to machine precision, the same solution in  $T$ .

Parallel numerical experiments have been performed on the multi-core partition of the supercomputer Piz Daint of the Swiss national supercomputing centre (CSCS)<sup>3</sup>.

<sup>1</sup><https://bitbucket.org/zulianp/utopia>

<sup>2</sup><https://pfasst.lbl.gov/codes>

<sup>3</sup><https://www.cscs.ch/computers/piz-daint>

**5.2. Solvers specifics and notation.** We introduce some of the notation that we are going to use in the following numerical experiments:

- $\boxed{\text{STMG}_\nu^L}$   
Space-time multigrid with  $L$  levels with  $T_l^{l+1}$  and  $S_l^{l+1}$  in (4.1) being standard linear coarsening<sup>4</sup> in time and space and  $M_l^{l+1} = I_M$  for all  $l = 1, \dots, L-1$ , i.e.  $M$  is constant along the multilevel hierarchy. We use V-cycling, with  $\nu$  smoothing iterations of PGMRES. If multiple processors are used, an additional block Jacobi preconditioner is employed, using a single block for each parallel processor. On the coarsest level, an LU factorization is used and coarse problems are assembled through Galerkin assembly.
- $\boxed{\text{SMG}_\nu^L}$   
As  $\text{STMG}_\nu^L$ , but without temporal coarsening: time transfers are replaced by identities in (4.1), i.e.  $T_l^{l+1} = I_{N_t}$  for all  $l = 1, \dots, L-1$ .
- $\boxed{\text{SMMG}_\nu^L}$   
As  $\text{SMG}_\nu^L$ , but using  $M$ -coarsening in time; in (4.1)  $M_l^{l+1}$  is obtained through linear interpolation and the number of time nodes  $M$  is reduced progressively on the level hierarchy until  $M = 1$  is reached, i.e.  $M = \max\{M-l+1, 1\}$  on level  $l$ .
- $\boxed{\text{PFASST}_\nu^L}$   
PFASST solver, as described in Section 4.1, with  $L$  levels and  $\nu$  sweeps per level. We use PGMRES as a spatial solution method and standard bisection to create coarse spatial problems. Regarding temporal coarsening, for performance reasons, we use  $M = 1$  on all coarse levels.

In the numerical results the run-times are expressed in seconds; the assembly of discrete problems and transfer operators are not included in the run-times. The number of iterations to convergence, if present, is reported in square brackets. Convergence is reached when the relative or the absolute preconditioned residual is less than a tolerance of  $10^{-9}$ . The acronym “n.c.” stands for “not converged”, denoting an increasing residual or if 1000 iterations are exceeded. The tests are restricted to temporal parallelism, i.e.  $\#\text{Cores} \leq N_t$ , choosing *optimal* solvers parameters (i.e.  $L$  and  $\nu$ ) to minimize run-time for both approaches. Linear and non-linear iterative solvers are initialized with the zero vector in the space-time case. The spatial diffusion solvers in PFASST (PGMRES), are initialized with the best available guess, i.e. the solution at the previous time step.

**5.3. Linear example: the heat equation.** In this section we consider the heat equation, i.e. in the following experiments we set  $\gamma = 0$  in (3.1), and the initial condition is

$$(5.1) \quad u_0(x) = \cos(\pi x) + 2 \cos(3\pi x) + 3 \cos(4\pi x) \quad \text{for } x \in [0, X],$$

---

<sup>4</sup>Using the stencil  $[1 \ 2 \ 1]/4$ . The operator  $T_l^{l+1}$  (resp.  $S_l^{l+1}$ ) has size  $N_t/2^l \times N_t/2^{l+1}$  (resp.  $(1 + N_x/2^l) \times (1 + N_x/2^{l+1})$ ).

with the corresponding analytical solution

$$(5.2) \quad u(x, t) = \cos(\pi x)e^{-\pi^2 t} + 2 \cos(3\pi x)e^{-9\pi^2 t} + 3 \cos(4\pi x)e^{-16\pi^2 t}.$$

We also consider the analytical solution  $\tilde{u}$ , obtained after spatial discretization, to focus on the error introduced just by temporal discretization:

$$(5.3) \quad \tilde{u}(x, t) = \cos(\pi x)e^{\rho_1 t} + 2 \cos(3\pi x)e^{\rho_2 t} + 3 \cos(4\pi x)e^{\rho_3 t},$$

with

$$\rho_1 = (2 \cos(\pi h) - 2)/h^2, \quad \rho_2 = (2 \cos(3\pi h) - 2)/h^2, \quad \rho_3 = (2 \cos(4\pi h) - 2)/h^2.$$

We show, in Figure 5.1, how the error behaves as a function of the temporal discretization parameters, i.e.  $N_t$  and  $M$ . One can see from the left plot in Figure 5.1, that the error compared to the exact solution decreases as the number of time steps increases until the spatial error of roughly  $10^{-9}$  dominates. The right-hand plot shows that the temporal error decreases with correct order  $2M - 1$  until machine precision is reached.

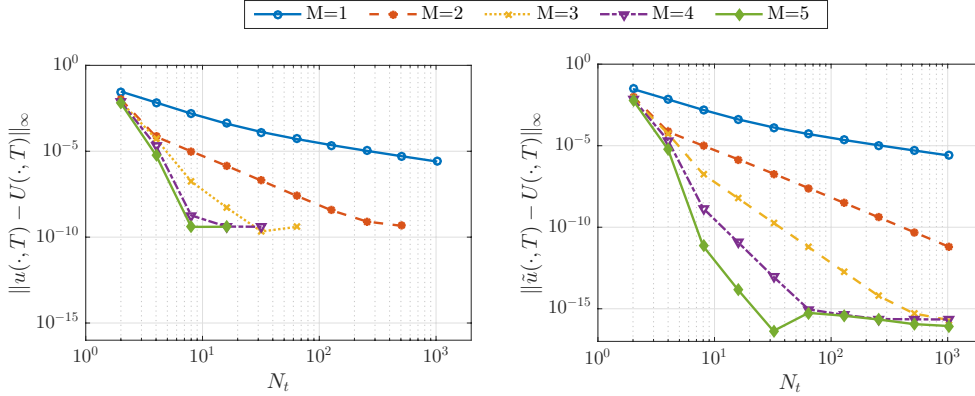


FIG. 5.1. Let us consider problem (3.1) with  $T = X = 1$ ,  $\gamma = 0$  and  $u_0$  from (5.1), discretized, according to (3.4) with  $N_x = 1024$ . Left: error at the end node w.r.t. the analytical solution (5.2). Right: error w.r.t. (5.3), i.e. the error of the discrete ODE. The two errors are until the spatial error dominates, and they decrease with the expected order  $(2M - 1)$ .

In Example 5.1-5.2 we report strong and weak scaling results varying the discretization order  $M$ .

EXAMPLE 5.1. (Strong scaling). Let us consider the continuous problem (3.1) with parameters  $X = T = 1$  and  $u_0$  from (5.1). We use the discretization parameters  $N_x = 1024$ ,  $M = \{1, \dots, 5\}$  and  $N_t$  varying according to the results of Figure 5.1, to avoid over-resolving in time. Just for  $M = 1$  we use  $N_t = 1024$ , with a corresponding accuracy of approximately  $10^{-6}$ .

We show, in Tables 5.1–5.3, run-times and iterations of the three multilevel approaches described in Section 5.2. The most relevant results are illustrated in Figure 5.2.



	STM $G_3^5$				
	$M = 1,$	$M = 2,$	$M = 3,$	$M = 4,$	$M = 5,$
Cores	$N_t = 1024$	$N_t = 256$	$N_t = 32$	$N_t = 16$	$N_t = 8$
1	2.72 [6]	4.13 [16]	3.78 [67]	5.26 [111]	n.c.
2	1.37 [6]	2.45 [20]	1.66 [61]	2.61 [115]	n.c.
4	1.28 [12]	2.15 [34]	0.94 [66]	1.59 [135]	n.c.
8	1.96 [34]	6.17 [175]	5.0 [680]	n.c.	n.c.
16	n.c.	7.38 [345]	n.c.	n.c.	
32	1.63 [61]	14.0 [907]	n.c.		
64	n.c.	3.11 [372]			
128	n.c.	3.47 [579]			
256	n.c.	5.48 [942]			
512	n.c.				
1024	n.c.				

TABLE 5.1

*Five level space-time multigrid run-times and iterations to convergence, with full space-time coarsening and n.c. abbreviating “not converged”.*

	SM $G_3^7$				
	$M = 1,$	$M = 2,$	$M = 3,$	$M = 4,$	$M = 5,$
Cores	$N_t = 1024$	$N_t = 256$	$N_t = 32$	$N_t = 16$	$N_t = 8$
1	1.67 [2]	1.35 [3]	0.32 [4]	0.27 [4]	0.29 [7]
2	1.14 [3]	0.72 [3]	0.23 [6]	0.13 [4]	0.09 [4]
4	0.95 [5]	0.59 [5]	0.14 [7]	0.07 [4]	0.06 [5]
8	0.65 [6]	0.45 [7]	0.12 [10]	0.10 [12]	0.07 [12]
16	0.43 [6]	0.22 [7]	0.07 [9]	0.05 [9]	
32	0.35 [7]	0.18 [8]	0.04 [8]		
64	0.13 [6]	0.08 [6]			
128	0.09 [6]	0.06 [6]			
256	0.07 [5]	0.06 [6]			
512	0.07 [5]				
1024	0.10 [5]				

TABLE 5.2

*Seven level space-time multigrid run-times and iterations to convergence with no temporal coarsening.*

Cores	SMMG <sub>3</sub> <sup>7</sup>			
	$M = 2,$ $N_t = 256$	$M = 3,$ $N_t = 32$	$M = 4,$ $N_t = 16$	$M = 5,$ $N_t = 8$
1	2.60 [14]	0.70 [21]	0.81 [29]	0.98 [45]
2	1.26 [14]	0.35 [21]	0.43 [29]	0.60 [45]
4	0.69 [14]	0.20 [21]	0.22 [29]	0.29 [45]
8	9.18 [382]	3.81 [788]	n.c.	n.c
16	8.35 [560]	2.19 [714]	n.c.	
32	8.43 [835]	n.c.		
64	1.64 [254]			
128	0.83 [172]			
256	0.34 [73]			

TABLE 5.3

Seven level space-time multigrid run-times and iterations to convergence, with  $M$ -coarsening in time. The column for  $M = 1$  is not present as it would be equivalent to the one of Table 5.2.

Cores	PFASST <sub>1</sub> <sup>3</sup>				
	$M = 1,$ $N_t = 1024$	$M = 2,$ $N_t = 256$	$M = 3,$ $N_t = 32$	$M = 4,$ $N_t = 16$	$M = 5,$ $N_t = 8$
1	1.49 [2]	0.74 [3]	0.23 [11]	0.17 [12]	0.12 [12]
2	1.26 [3]	0.71 [11]	0.17 [14]	0.12 [14]	0.09 [15]
4	0.85 [4]	0.50 [13]	0.11 [16]	0.08 [17]	0.06 [18]
8	0.55 [6]	0.40 [17]	0.09 [20]	0.07 [21]	0.05 [22]
16	0.37 [7]	0.31 [24]	0.08 [28]	0.06 [29]	
32	0.23 [7]	0.21 [29]	0.06 [35]		
64	0.18 [7]	0.15 [30]			
128	0.15 [8]	0.11 [30]			
256	0.15 [7]	0.11 [30]			
512	0.16 [8]				
1024	0.20 [7]				

TABLE 5.4

Three level PFASST run-times and iterations to convergence.

We can describe the discretization settings of Example 5.1 through the parameter

$$\mu = \frac{\Delta t}{\Delta x^2} = \frac{N_x^2}{N_t}.$$

In all cases considered  $\mu \gg 1$ ; from space-time multigrid literature, e.g. [21], we can expect time coarsening to be not effective in this scenario, as we observe from Table 5.1 and Table 5.3.

EXAMPLE 5.2. (*Weak time scaling in  $N_t$* ) Let us consider the continuous problem (3.1) with parameters  $X = T = 1$  and  $u_0$  from (5.1). We use the discretization parameters  $N_x = 1024$ ,  $M = \{1, \dots, 5\}$  and  $N_t = C_M \cdot \text{Cores}$ . The parameter  $C_M$  depends on  $M$  and is chosen according to the parallel saturation from Example 5.1; for example, for  $M = 1$  and  $N_t = 1024$ , according to Tables 5.2–5.4, we have maximum speedup with 256 cores and therefore  $C_1 = 4$ . Similarly  $C_2 = 2$  and  $C_M = 1$  for  $M \geq 3$ . We point out that the accuracy of the solution as a function of  $N_t$  is varying in the tables according to Figure 5.1: doubling  $N_t$  corresponds to an higher accuracy as  $M$  increases. We report, in Tables 5.5–5.6 and Figure 5.3 run-times and iterations of the multilevel approaches described in Section 5.2. It is clear from Figure 5.3 that the higher-order methods display better weak scaling than the lower order methods, but this is partly due to the fact that the overall error in the solution as  $N_t$  increases becomes exceedingly small.

$M = 1$				$M = 2$			
Cores	$N_t$	time [its.]	$R$	Cores	$N_t$	time [its.]	$R$
256	1024	0.09 [5]	1	128	256	0.06 [6]	1.0
512	2048	0.20 [5]	2.2	256	512	0.11 [5]	1.8
1024	4096	0.37 [5]	4.1	512	1024	0.21 [5]	3.5
2048	8192	0.62 [5]	6.9	1024	2048	0.37 [5]	6.2

$M = 3$				$M = 4$			
Cores	$N_t$	time [its.]	$R$	Cores	$N_t$	time [its.]	$R$
32	32	0.04 [8]	1.0	16	16	0.04 [9]	1.0
64	64	0.04 [5]	1.0	32	32	0.05 [9]	1.2
128	128	0.05 [6]	1.2	64	64	0.05 [6]	1.2
256	256	0.07 [5]	1.7	128	128	0.07 [6]	1.7

$M = 5$			
Cores	$N_t$	time [its.]	$R$
8	8	0.08 [12]	1.0
16	16	0.09 [12]	1.1
32	32	0.11 [10]	1.4
64	64	0.10 [6]	1.2

TABLE 5.5

Weak scaling in time of a seven level space-time multigrid  $SMG_7^3$ , with no temporal coarsening. The ratio  $R$  is computed dividing the current run-time by the base one (in the first line for each table) and  $R = 1$  denotes an ideal weak scaling.

$M = 1$				$M = 2$			
Cores	$N_t$	time [its.]	$R$	Cores	$N_t$	time [its.]	$R$
256	1024	0.16 [7]	1.0	128	256	0.09 [30]	1.0
512	2048	0.26 [8]	1.6	256	512	0.11 [30]	1.2
1024	4096	0.49 [10]	3.1	512	1024	0.16 [29]	1.8
2048	8192	0.96 [10]	6.0	1024	2048	0.25 [30]	2.8

$M = 3$				$M = 4$			
Cores	$N_t$	time [its.]	$R$	Cores	$N_t$	time [its.]	$R$
32	32	0.06 [35]	1.0	16	16	0.07 [29]	1.0
64	64	0.11 [38]	1.8	32	32	0.10 [38]	1.4
128	128	0.12 [38]	2.0	64	64	0.12 [42]	1.4
256	256	0.13 [36]	2.2	128	128	0.12 [42]	1.7

$M = 5$			
Cores	$N_t$	time [its.]	$R$
8	8	0.05 [22]	1.0
16	16	0.08 [30]	1.6
32	32	0.10 [39]	2.0
64	64	0.11 [42]	2.2

TABLE 5.6

Weak scaling in time of  $\text{PFASST}_1^3$ . The ratio  $R$  is computed dividing the current run-time by the base one (in the first line for each table) and  $R = 1$  denotes an ideal weak scaling. We can notice that the weak scaling for  $M = 1$  is poor, since no temporal coarsening is present in this case.

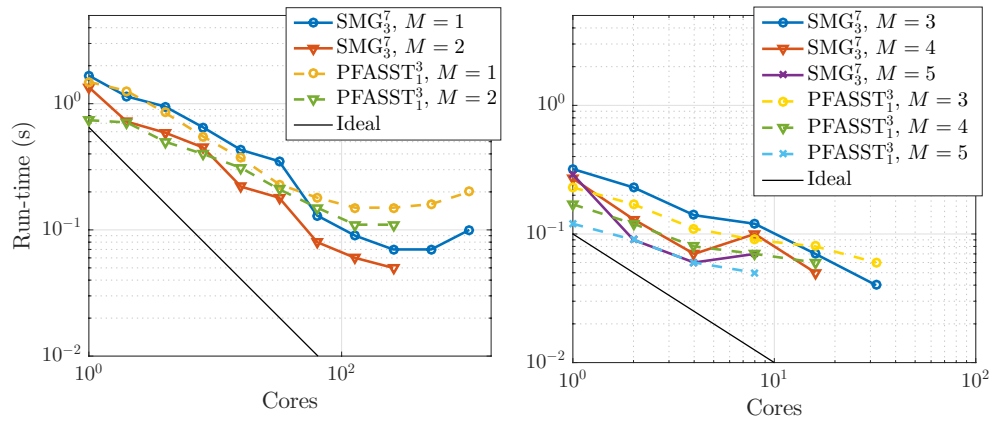


FIG. 5.2. Strong scaling timing results of SMG (solid lines) and PFASST (dashed lines) from Example 5.1; run-times of STMG and SMMG are not included since they are not competitive. We report run-times for  $M \in \{1, 2\}$  in the left plot and for  $M \in \{3, 4, 5\}$  in the right one.

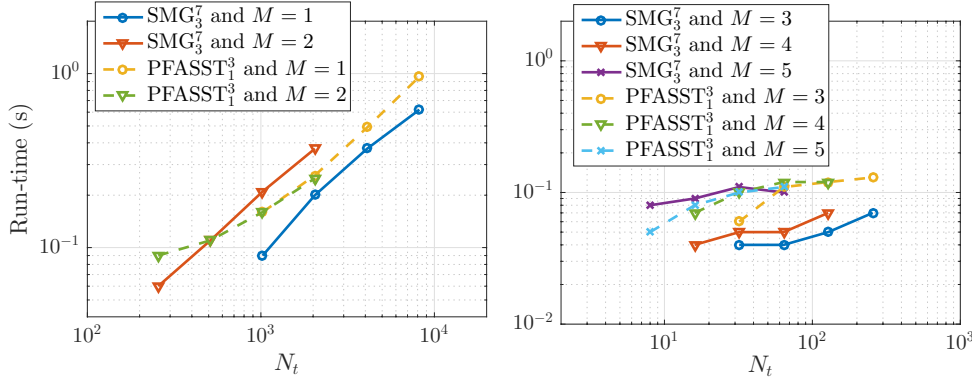


FIG. 5.3. Weak scaling timing results of SMG (solid lines) and PFASST (dashed lines) from Tables 5.5–5.6; run-times of STMG and SMMG are not included since they are not competitive. We report run-times for  $M \in \{1, 2\}$  in the left plot and for  $M \in \{3, 4, 5\}$  in the right one.

**5.4. Non-linear example: the monodomain equation..** In this section we consider the full reaction-diffusion model, i.e.  $\gamma > 0$  in (3.1). We remark that, for the space-time discretization in (3.4), a non-linear solver is required for both the implicit or the explicit treatment of the cubic reaction term. In this sense PFASST, is more flexible as it allows an IMEX setting.

To model a traveling wave in an excitable media we consider reaction dominated examples. In this case we set a narrow initial stimulus in the centre of the domain and we chose  $T$  such that the final solution is stationary, i.e. for all  $x$  we have  $u(T, x) \simeq 1$  and  $\partial_t u(T, x) \simeq 0$ .

EXAMPLE 5.3. (Strong scaling) Let us consider the continuous problem (3.1) with model parameters  $X = 10, T = 2, \gamma = 5$  and the initial condition

$$u_0 = 2 \exp \left( \frac{(x - X)^2}{0.1} \right).$$

We use the discretization parameters  $N_x = N_t = 1024$  and  $M = \{1, \dots, 5\}$ . We show, in Table 5.7, run-times and Newton iterations of the space-time strategy, using  $SMG_3^7$  as linear solver and, in Table 5.8, the PFASST data.

Note that in the cases where PFASST converges, the run time is significantly smaller than the corresponding SMG times. This is due to the fact that the PFASST implementation is using a semi-implicit or IMEX time stepping method, so that the cost per iteration is essentially the same as for the heat equation example. On the other hand, the SMG method is fully implicit and nonlinear requiring Newton iterations. The failure of PFASST to converge for large time steps is also due to the IMEX stepping, which has a time step restriction due to the explicit treatment of the reaction term (see, e.g. [38]). The reaction term could also be handled implicitly using a multi-implicit approach [10] as was done in [25], but we defer this sort of comparison to future work.

	SMG <sub>3</sub> <sup>7</sup>				
	$M = 1,$	$M = 2,$	$M = 3,$	$M = 4,$	$M = 5,$
Cores	$N_t = 1024$	$N_t = 256$	$N_t = 32$	$N_t = 16$	$N_t = 8$
1	46.4 [16]	31.1 [16]	6.47 [16]	5.18 [16]	301 [58]
2	29.7 [16]	19.5 [16]	4.50 [16]	3.75 [16]	123 [45]
4	16.6 [16]	11.0 [16]	2.61 [16]	2.17 [16]	125 [47]
8	10.6 [16]	7.45 [16]	1.81 [16]	1.60 [16]	34.4 [18]
16	8.51 [16]	5.81 [16]	1.36 [16]	1.16 [16]	
32	7.22 [16]	4.92 [16]	1.07 [16]		
64	6.11 [16]	4.54 [16]			
128	5.10 [16]	3.90 [16]			
256	5.50 [16]	5.48 [16]			
512	5.64 [16]				
1024	6.20 [16]				

TABLE 5.7

*Run-time of a seven level space-time multigrid, with no temporal coarsening and corresponding Newton iterations.*

	PFASST <sub>1</sub> <sup>3</sup>				
	$M = 1,$	$M = 2,$	$M = 3,$	$M = 4,$	$M = 5,$
Cores	$N_t = 1024$	$N_t = 256$	$N_t = 32$	$N_t = 16$	$N_t = 8$
1	1.51 [2]	0.54 [5]	0.23 [93]	n.c.	n.c.
2	1.16 [3]	0.42 [6]	0.20 [94]	n.c.	n.c.
4	0.67 [4]	0.25 [8]	n.c.	n.c.	n.c.
8	0.40 [5]	0.16 [8]	n.c.	n.c.	n.c.
16	0.27 [6]	0.11 [8]	n.c.	n.c.	
32	0.18 [6]	0.07 [8]	n.c.		
64	0.14 [6]	0.07 [8]			
128	0.13 [6]	0.07 [8]			
256	0.15 [6]	0.08 [8]			
512	0.16 [6]				
1024	0.20 [6]				

TABLE 5.8

*Three level PFASST run-times and iterations.*

**6. Conclusions.** We reported the parallel performance of multilevel space-time solution strategies and of the algorithm PFASST for a (reaction) diffusion problem.

From an implementation prospective, space-time multigrid approaches are convenient since the time parallelization boils down to the parallel solution of a system of equations (in (3.4)), for example using fast and parallel preconditioned Krylov methods as PGMRES. A tensor structure between space and time grids allows for a flexible choice of coarsening strategies, since transfer operators in (4.1) can be set

independently. On the other hand, the assembly of system (3.4) comes at a cost, in terms of time and, especially, memory footprint. Such cost can be reduced significantly when (3.4) is distributed among many processors and if highly parallel assembly routines are used, as parallel Kronecker products in (3.5).

In Examples 5.1–5.2 we investigated the scalability of different parallel iterative strategies for a diffusion problem. We obtained similar performance from PFASST and the parallel space-time multigrid with no temporal coarsening (SMG). The use of high order methods in time, reducing the number of time steps  $N_t$  accordingly, is convenient for both approaches, in terms of overall performance and especially for the weak scaling in time.

As expected from the literature, full space-time coarsening or time coarsening are not effective in the settings we considered ( $\mu \gg 1$ ). In the space-time multigrid framework  $M$ –coarsening in time can be advantageous w.r.t. coarsening in the number of time steps  $N_t$ , in terms of stability, but employing just coarsening in space remains the best option for the discretizations considered.

In Example 5.3 we considered a non-linear reaction-diffusion problem. For such a problem the space-time approach is limited to a fully implicit treatment of the non-linearity and the corresponding use of a non-linear solver, such as Newton’s method. In particular, we observe that the number of Newton iterations to convergence is not robust in terms of problem parameters and initial guess. On the other hand, in this respect PFASST is more flexible since it allows to treat the non-linearity explicitly, through an IMEX approach. Such a strategy, even if less stable (especially for large  $\Delta t$  and high order  $M$ ), can reduce dramatically the time-to-solution.

**Acknowledgements.** The authors acknowledge the Deutsche Forschungsgemeinschaft (DFG) as part of the “ExaSolvers” Project in the Priority Programme 1648 “Software for Exascale Computing” (SPPEXA) and the Swiss National Science Foundation (SNSF) under the lead agency grant agreement SNSF-162199. The work of M. Minion was supported by the U.S. Department of Energy, Office of Science, Office of Advanced Scientific Computing Research, Applied Mathematics program under contract number DE-AC02005CH11231

## REFERENCES

- [1] S. BALAY, S. ABHYANKAR, M. F. ADAMS, J. BROWN, P. BRUNE, K. BUSCHELMAN, L. DALCIN, A. DENER, V. ELJKHOUT, W. D. GROPP, D. KARPEYEV, D. KAUSHIK, M. G. KNEPLEY, D. A. MAY, L. C. MCINNES, R. T. MILLS, T. MUNSON, K. RUPP, P. SANAN, B. F. SMITH, S. ZAMPINI, H. ZHANG, AND H. ZHANG, *PETSc users manual*, Tech. Report ANL-95/11 - Revision 3.12, Argonne National Laboratory, 2019, <https://www.mcs.anl.gov/petsc>.
- [2] S. BALAY, S. ABHYANKAR, M. F. ADAMS, J. BROWN, P. BRUNE, K. BUSCHELMAN, L. DALCIN, A. DENER, V. ELJKHOUT, W. D. GROPP, D. KARPEYEV, D. KAUSHIK, M. G. KNEPLEY, D. A. MAY, L. C. MCINNES, R. T. MILLS, T. MUNSON, K. RUPP, P. SANAN, B. F. SMITH, S. ZAMPINI, H. ZHANG, AND H. ZHANG, *PETSc Web page*, <https://www.mcs.anl.gov/petsc>, 2019, <https://www.mcs.anl.gov/petsc>.
- [3] P. BENEDUSI, *Parallel space-time multilevel methods with application to electrophysiology*, PhD thesis, Università della Svizzera italiana, 2020.
- [4] P. BENEDUSI, P. FERRARI, C. GARONI, R. KRAUSE, AND S. SERRA-CAPIZZANO, *Fast parallel solver for the space-time IgA-DG discretization of the anisotropic diffusion equation*, 2019.
- [5] P. BENEDUSI, C. GARONI, R. KRAUSE, X. LI, AND S. SERRA-CAPIZZANO, *Space-time FE-DG*

- discretization of the anisotropic diffusion equation in any dimension: The spectral symbol*, SIAM Journal on Matrix Analysis and Applications, 39 (2018), pp. 1383–1420.
- [6] P. BENEDUSI, D. HUPP, P. ARBENZ, AND R. KRAUSE, *A parallel multigrid solver for time-periodic incompressible Navier-Stokes equations in 3D*, in Numerical Mathematics and Advanced Applications ENUMATH 2015, Springer, 2016, pp. 265–273.
  - [7] M. BESIER AND R. RANNACHER, *Goal-oriented spacetime adaptivity in the finite element Galerkin method for the computation of nonstationary incompressible flow*, International Journal for Numerical Methods in Fluids, 70 (2012), pp. 1139–1166, <https://doi.org/10.1002/fld.2735>.
  - [8] M. BOLTEN, D. MOSER, AND R. SPECK, *A multigrid perspective on the parallel full approximation scheme in space and time*, Numerical Linear Algebra with Applications, 24 (2017), p. e2110.
  - [9] S. BÖRM AND R. HIPTMAIR, *Analysis of tensor product multigrid*, Numerical Algorithms, 26 (2001), pp. 219–234.
  - [10] A. BOURLIOUX, A. T. LAYTON, AND M. L. MINION, *High-order multi-implicit spectral deferred correction methods for problems of reactive flow*, J. Comput. Phys., 189 (2003), pp. 651–675.
  - [11] W. L. BRIGGS, V. E. HENSON, AND S. F. MCCORMICK, *A Multigrid Tutorial*, SIAM, Philadelphia, 2nd ed., 2000.
  - [12] M. DELFOUR, W. HAGER, AND F. TROCHU, *Discontinuous Galerkin methods for ordinary differential equations*, Mathematics of Computation, 36 (1981), pp. 455–473.
  - [13] A. DUTT, L. GREENGARD, AND V. ROKHLIN, *Spectral deferred correction methods for ordinary differential equations*, BIT Numerical Mathematics, 40 (2000), pp. 241–266.
  - [14] M. EMMETT AND M. L. MINION, *Toward an efficient parallel in time method for partial differential equations*, Communications in Applied Mathematics and Computational Science, 7 (2012), pp. 105–132, <http://dx.doi.org/10.2140/camcos.2012.7.105>.
  - [15] K. ERIKSSON AND C. JOHNSON, *Adaptive finite element methods for parabolic problems i: A linear model problem*, SIAM Journal on Numerical Analysis, 28 (1991), pp. 43–77.
  - [16] K. ERIKSSON AND C. JOHNSON, *Adaptive finite element methods for parabolic problems ii: Optimal error estimates in  $L_\infty L_2$  and  $L_\infty L_\infty$* , SIAM Journal on Numerical Analysis, 32 (1995), pp. 706–740.
  - [17] K. ERIKSSON, C. JOHNSON, AND V. THOMÉE, *Time discretization of parabolic problems by the discontinuous Galerkin method*, ESAIM: Mathematical Modelling and Numerical Analysis, 19 (1985), pp. 611–643.
  - [18] R. D. FALGOUT, S. FRIEDHOFF, T. V. KOLEV, S. P. MACLACHLAN, AND J. B. SCHRODER, *Parallel time integration with multigrid*, SIAM Journal on Scientific Computing, 36 (2014), pp. C635–C661, <http://dx.doi.org/10.1137/130944230>.
  - [19] R. D. FALGOUT, S. FRIEDHOFF, T. V. KOLEV, S. P. MACLACHLAN, J. B. SCHRODER, AND S. VANDEWALLE, *Multigrid methods with space-time concurrency*, Computing and Visualization in Science, 18 (2017), pp. 123–143.
  - [20] M. FEISTAUER, V. KUČERA, K. NAJZAR, AND J. PROKOPOVÁ, *Analysis of space-time discontinuous Galerkin method for nonlinear convection-diffusion problems*, Numerische Mathematik, 117 (2011), pp. 251–288.
  - [21] S. R. FRANCO, F. J. GASPAR, M. A. V. PINTO, AND C. RODRIGO, *Multigrid method based on a space-time approach with standard coarsening for parabolic problems*, Applied Mathematics and Computation, 317 (2018), pp. 25–34.
  - [22] M. J. GANDER, *50 years of time parallel time integration*, in Multiple Shooting and Time Domain Decomposition, Springer, 2015, [http://dx.doi.org/10.1007/978-3-319-23321-5\\_3](http://dx.doi.org/10.1007/978-3-319-23321-5_3).
  - [23] M. J. GANDER, F. KWOK, AND H. ZHANG, *Multigrid interpretations of the parareal algorithm leading to an overlapping variant and mgrit*, Computing and Visualization in Science, 19 (2018), pp. 59–74.
  - [24] M. J. GANDER AND M. NEUMÜLLER, *Analysis of a new space-time parallel multigrid algorithm for parabolic problems*, SIAM Journal on Scientific Computing, 38 (2016), pp. A2173–A2208.
  - [25] S. GÖTSCHEL AND M. L. MINION, *An efficient Parallel-in-Time method for optimization with parabolic PDEs*, SIAM J. Sci. Comput., 41 (2019), pp. C603–C626.
  - [26] W. HACKBUSCH, *Parabolic multi-grid methods*, Computing Methods in Applied Sciences and



- Engineering, VI, (1984), pp. 189–197, <http://dl.acm.org/citation.cfm?id=4673.4714>.
- [27] E. E. HAIRER AND G. WANNER, *Solving ordinary differential equations II : stiff and differential-algebraic problems*, Springer Berlin Heidelberg, 1991.
  - [28] C. HOFER, U. LANGER, M. NEUMÜLLER, AND R. SCHNECKENLEITNER, *Parallel and robust preconditioning for space-time isogeometric analysis of parabolic evolution problems*, SIAM Journal on Scientific Computing, 41 (2019), pp. A1793–A1821.
  - [29] G. HORTON AND S. VANDEWALLE, *A Space-Time Multigrid Method for Parabolic Partial Differential Equations*, SIAM Journal on Scientific Computing, 16 (1995), pp. 848–864, <http://dx.doi.org/10.1137/0916050>.
  - [30] J. HUANG, J. JIA, AND M. MINION, *Accelerating the convergence of spectral deferred correction methods*, J. Comput. Phys., 214 (2006), pp. 633–656.
  - [31] S. HUSSAIN, F. SCHIEWECK, AND S. TUREK, *Higher order Galerkin time discretizations and fast multigrid solvers for the heat equation*, Journal of Numerical Mathematics, 19 (2011), pp. 41–61.
  - [32] P. JAMET, *Galerkin-type approximations which are discontinuous in time for parabolic equations in a variable domain*, SIAM Journal on Numerical Analysis, 15 (1978), pp. 912–928.
  - [33] J. P. KEENER AND J. SNEYD, *Mathematical physiology*, vol. 1, Springer, 1998.
  - [34] C. KLAUJ, J. VAN DER VEGT, AND H. VAN DER VEN, *Space-time discontinuous Galerkin method for the compressible Navier-Stokes equations*, Journal of Computational Physics, 217 (2006), pp. 589 – 611.
  - [35] P. LASAINT AND P. RAVIART, *On a finite element method for solving the neutron transport equation*, in Mathematical Aspects of Finite Elements in Partial Differential Equations, Proceedings of a Symposium Conducted by the Mathematics Research Center, the University of Wisconsin-Madison, Madison, WI, USA, 1974, pp. 1–3.
  - [36] X. LI AND N.-E. WIBERG, *Implementation and adaptivity of a space-time finite element method for structural dynamics*, Computer Methods in Applied Mechanics and Engineering, 156 (1998), pp. 211–229.
  - [37] E. McDONALD AND A. WATHEN, *A simple proposal for parallel computation over time of an evolutionary process with implicit time stepping*, in Numerical Mathematics and Advanced Applications ENUMATH 2015, Springer, 2016, pp. 285–293.
  - [38] M. L. MINION, *Semi-implicit projection methods for incompressible flow based on spectral deferred corrections*, Appl. Numer. Math., 48 (2004), pp. 369–387.
  - [39] W. PAZNER AND P.-O. PERSSON, *Approximate tensor-product preconditioners for very high order discontinuous Galerkin methods*, Journal of Computational Physics, 354 (2018), pp. 344–369.
  - [40] T. RICHTER, A. SPRINGER, AND B. VEXLER, *Efficient numerical realization of discontinuous Galerkin methods for temporal discretization of parabolic problems*, Numerische Mathematik, 124 (2013), pp. 151–182.
  - [41] F. SCHIEWECK, *A-stable discontinuous Galerkin–petrov time discretization of higher order*, Journal of Numerical Mathematics, 18 (2010), pp. 25–57.
  - [42] M. SCHMICH AND B. VEXLER, *Adaptivity with dynamic meshes for space-time finite element discretizations of parabolic equations*, SIAM Journal on Scientific Computing, 30 (2008), pp. 369–393, <https://doi.org/10.1137/060670468>.
  - [43] D. SCHÖTZAU AND T. P. WIHLE, *A posteriori error estimation for hp-version time-stepping methods for parabolic partial differential equations*, Numerische Mathematik, 115 (2010), pp. 475–509.
  - [44] C.-W. SHU, *Discontinuous Galerkin method for time-dependent problems: survey and recent developments*, Springer International Publishing, 2014, pp. 25–62.
  - [45] I. SMEARS, *Robust and efficient preconditioners for the discontinuous Galerkin time-stepping method*, IMA Journal of Numerical Analysis, 37 (2016), pp. 1961–1985.
  - [46] R. SPECK, D. RUPRECHT, M. EMMETT, M. L. MINION, M. BOLTE, AND R. KRAUSE, *A multi-level spectral deferred correction method*, BIT Numerical Mathematics, 55 (2015), pp. 843–867.
  - [47] J. SUDIRHAM, J. VAN DER VEGT, AND R. VAN DAMME, *Space-time discontinuous Galerkin method for advection-diffusion problems on time-dependent domains*, Applied Numerical Mathematics, 56 (2006), pp. 1491 – 1518.
  - [48] V. THOMÉE, *Galerkin finite element methods for parabolic problems*, vol. 1054, Springer, 1984.

- [49] M. WEISER, *Faster sdc convergence on non-equidistant grids by dirk sweeps*, BIT Numerical Mathematics, 55 (2015), pp. 1219–1241.
- [50] S. ZHAO AND G.-W. WEI, *A unified discontinuous Galerkin framework for time integration*, Mathematical methods in the applied sciences, 37 (2014), pp. 1042–1071.
- [51] P. ZULIAN, A. KOPANIČÁKOVÁ, M. C. G. NESTOLA, A. FINK, N. FADEL, A. RIGAZZI, V. MAGRI, T. SCHNEIDER, E. BOTTER, J. MANKAU, AND R. KRAUSE, *Utopia: A C++ embedded domain specific language for scientific computing. Git repository*. <https://bitbucket.org/zulianp/utopia>, 2016, <https://bitbucket.org/zulianp/utopia>.